Chinese Chemical Letters 33 (2022) 2522–2526

Contents lists available at ScienceDirect

Chinese Chemical Letters

journal homepage: www.elsevier.com/locate/cclet

Mononuclear aggregation-induced emission (AIE)-active gold(I)-isocyanide phosphors: Contrasting phosphorescent mechanochromisms and effect of halogen substitutions on room-temperature phosphorescence nature

Xiaoyan Wang[a], Zhao Chen[a,b,*], Jun Yin[a], Sheng Hua Liu[a,c,*]

[a] Key Laboratory of Pesticide and Chemical Biology, Ministry of Education, College of Chemistry, Central China Normal University, Wuhan 430079, China
[b] Jiangxi Key Laboratory of Organic Chemistry, Jiangxi Science and Technology Normal University, Nanchang 330013, China
[c] State Key Laboratory of Structural Chemistry, Fujian Institute of Research on the Structure of Matter, Chinese Academy of Sciences, Fuzhou 350002, China

ARTICLE INFO

Article history:
Received 8 August 2021
Revised 11 December 2021
Accepted 13 December 2021
Available online 17 December 2021

Keywords:
Gold(I) complexes
Halogen atoms
Room temperature phosphorescence
Aggregation-induced emission
Phosphorescent mechanochromism

ABSTRACT

Developing phosphors with long-lifetime (millisecond scale or even longer) solid state room temperature phosphorescence (RTP) feature has attracted considerable attention. However, to date, stimuli-responsive phosphors with RTP nature are still rare due to the absence of effective guidelines for the exploitation of luminophors synchronously possessing stimuli-responsive and RTP characteristics. In this work, a series of mononuclear gold(I) complexes are reported. All these complexes exhibit various solid-state RTP properties, and phosphor **1-Cl** exhibits long-lived RTP behavior. The effect of halogen atoms on the RTP nature of these complexes is investigated in detail. Furthermore, the introduction of different types of halogen atoms can effectively regulate the phosphorescent mechanochromism phenomena of these gold(I)-containing complexes. In addition, these phosphors display typical aggregation-induced emission (AIE) effect except for phosphor **5-CCl**, which lacks hydrogen-bonding interactions compared with the other four phosphors. This work will be very helpful to the development of mechanical-force-responsive AIE phosphors with lasting RTP.

Luminescent materials are widely used in many fields, including in optoelectronic devices, sensors, and biological imaging [1–8]. Generally, luminescent materials are applied in the form of a solid thick or thin film; however, conventional fluorescent molecules only display emission in dilute solutions, and their emission intensity is markedly suppressed in the aggregated state. This phenomenon is referred to as the aggregation-caused quenching (ACQ) effect. In 2001, Luo *et al.* reported the first molecule with the opposite fluorescence characteristics, *i.e.*, aggregation-induced emission (AIE) [9]. Free rotors are usually introduced into AIE molecules to prevent the formation of π-π interactions, or rigid environments are created *via* intermolecular or intramolecular hydrogen-bonding interactions. These methods can suppress non-radiative transitions of the molecules in the aggregation states [10–13]. The unique AIE effects enable molecules that can overcome the limitations of conventional fluorescent molecules and greatly expand their application prospects [14,15].

Mechanochromic materials are ones that respond with a change in luminous intensity or color when stimulated by an external mechanical force [16–26]. Liao *et al.* explored the effect of the crystal packing mode of the molecules on their mechanoluminescence [27–29]. They reported that the molecular packing modes and degree of packing density were crucial factors affecting the emission properties. Moreover, the transition between a highly ordered crystalline state and the amorphous state is another important factor for mechanochromic materials [30–34]. Such materials have potential application prospects in the fields of force sensors, data storage, and anti-counterfeiting because of their simple operation and rapid response [35,36]. Transition metal complexes have become a topic of intense research interest in the field of luminescent materials because of their rich excited states and excellent photophysical properties, such as an easily tunable emission wavelength, long decay lifetime, and stable chemical structure [37–41]. The introduction of metal atoms also improves the rate of in-

* Corresponding authors at: Key Laboratory of Pesticide and Chemical Biology, Ministry of Education, College of Chemistry, Central China Normal University, Wuhan 430079, China.
E-mail addresses: chenzhao666@126.com (Z. Chen), chshliu@mail.ccnu.edu.cn (S.H. Liu).

https://doi.org/10.1016/j.cclet.2021.12.030
1001-8417/

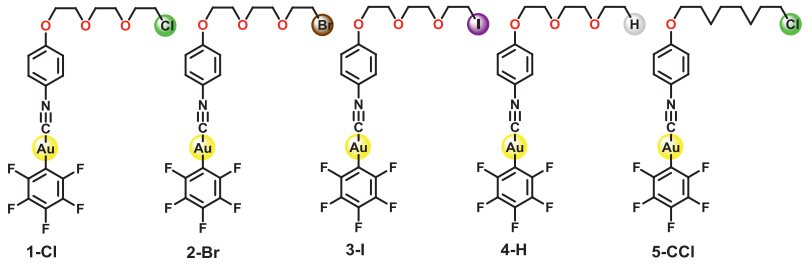

Scheme 1. Structures of gold(I) complexes.

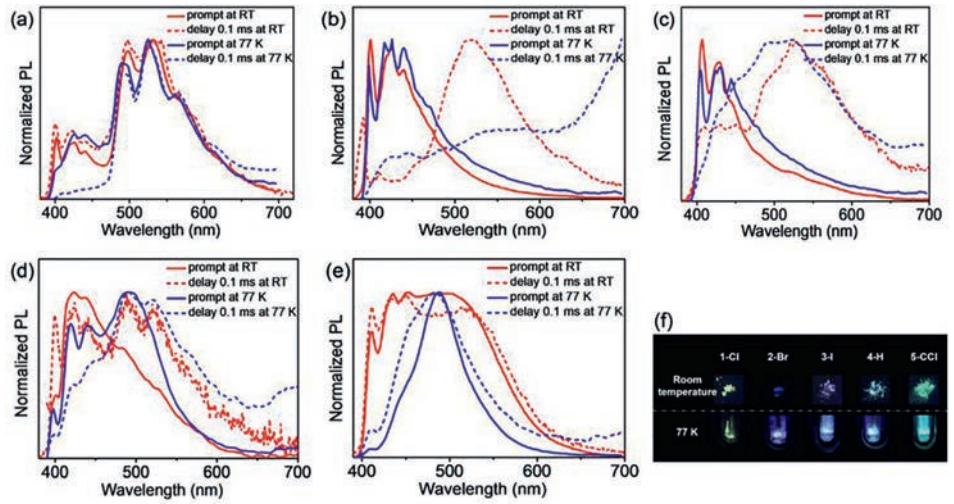

Fig. 1. Normalized steady-state (solid line) and delayed (dotted line) emission spectra of gold(I) complexes **1-Cl** (a), **2-Br** (b), **3-I** (c), **4-H** (d), **5-CCl** (e) at room temperature (red line) and 77 K (blue line). (f) The photographs of solids (taken at room temperature (above) and 77 K (below) under a 365 nm portable UV lamp).

tersystem crossing and luminescence lifetime. Many metal complexes with room temperature phosphorescence (RTP) properties have been reported [42–44]. However, there have been few reports on metal complexes with mechanochromism, AIE, and RTP. To address this, systematically studying the relationship between the structures and properties of these multifunctional complexes is essential for designing novel metal complexes with the desired functionalities. According to previous reports, altering the gold-gold distance is important for regulating the emission properties of Au complexes [45–48]. Therefore, gold atoms were introduced in the molecules to enhance the electronic interaction between complexes. The halogen atoms, Cl, Br, and I were also modified at the ends of the complexes; this was expected to increase the rate of intersystem crossing and allow for systematic investigation of the effect of different halogen atoms on the luminescent properties. Furthermore, flexible oxygen-rich tetraethylene glycol(TEG)-like side chains have been introduced to enhance the intermolecular hydrogen bonding interactions and provide a rigid environment for the construction of AIE molecules. In this work, the halogen-containing gold(I) complexes **1-Cl**, **2-Br** and **3-I** (Scheme 1) were designed and synthesized. In addition, the complexes **4-H** and **5-CCl** (Scheme 1) were also studied for comparison. The design strategies proposed in this paper synchronously explored the effects of both structural modification and intermolecular interactions on the room-temperature phosphorescent lifetimes, mechanochromism, and aggregation-induced emission properties.

The structures of the target complexes are shown in Scheme 1, and their detailed synthetic routes are shown in supporting information (Scheme S1 in Supporting information). All the gold(I) complexes were confirmed by NMR and mass spectrometry. The crystal structures of **1-Cl**, **2-Br**, **3-I** and **4-H** were obtained by slow evaporation in a dichloromethane/*n*-hexane solution.

To investigate the luminescent characteristics of complexes **1-Cl**, **2-Br**, **3-I**, **4-H** and **5-CCl**, the emission spectra of these gold(I) complexes in the solid states were firstly studied, including the steady-state and delayed spectra at room temperature and at 77 K (Fig. 1). Taking **1-Cl** as an example, the steady-state spectrum at room temperature showed two groups of emission peaks located in the range of 400–460 nm and 480–600 nm, showing yellow-green emission. The delayed spectrum was collected by exciting the sample with UV light and detecting the emission after 0.1 ms. It was found that the two groups of emission peaks were still present [49], which indicated that the lifetimes at both the short and long wavelengths were sufficiently long lived. When the sample was cooled to 77 K environment, it was found that the steady-state spectrum still had two groups of emission peaks, and the positions were basically the same as the steady-state spectrum obtained at room temperature. The delayed emission spectrum at 77 K was also tested. As shown in Fig. 1a, the emission peaks at short wavelengths disappeared, and only the long-wavelength emission signal remained. In contrast, the luminescence of the two other halogen-containing gold(I) complexes (**2-Br** and **3-I**) differed from that of the **1-Cl**. At room temperature, the steady-state spectra of **2-Br** and **3-I** showed multiple emission peaks between 400 nm and 460 nm, exhibiting blue and purple light, respectively. After a delay of 0.1 ms, new strong emission peaks appeared at ~520 nm, and the emission intensity at short wavelengths weakened or even disappeared. The steady-state spectra at 77 K were basically the same as that at room temperature; however, in the delayed spectra at 77 K, the emission peaks were mainly distributed in the long-wavelength range. Similarly, compared with the steady-state spectrum at room temperature, the relative intensity of the long-wavelength emission was greatly enhanced in the delayed spectrum for **4-H**, and it was further enhanced in the steady-state and

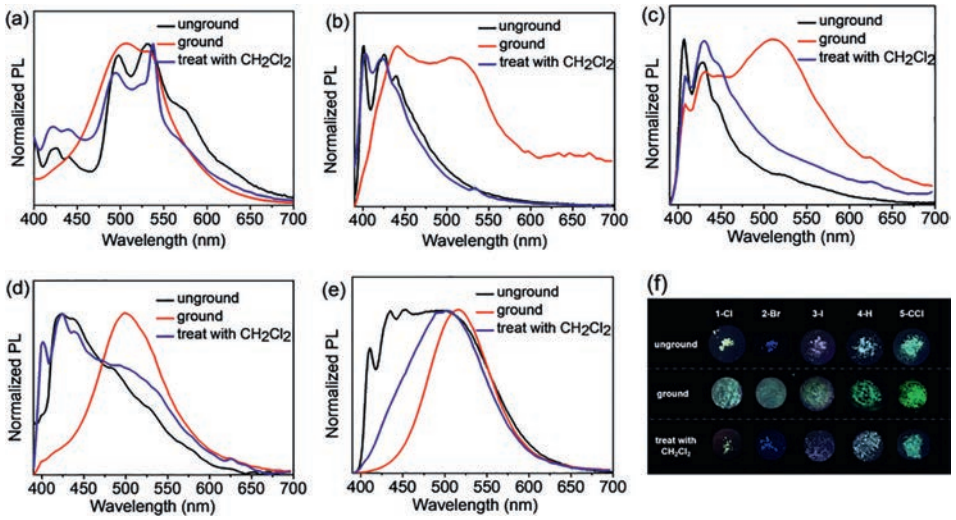

Fig. 2. Normalized emission spectra for **1-Cl** (a), **2-Br** (b), **3-I** (c), **4-H** (d), **5-CCl** (e) in different states (unground, ground, treat with CH_2Cl_2). (f) Photographs of gold(I) complexes in different situations taken under the 365 nm UV lamp.

delayed spectra at 77 K. The emission of **5-CCl** was completely different from that of **1-Cl**, although their structures differed by only two oxygen atoms in the flexible chain. For **5-CCl**, both the steady-state and delayed spectra showed broad emission peaks covering a range 400–700 nm at room temperature, while a narrow emission peak was observed at ~486 nm at 77 K. This indicated that the oxygen atoms in the flexible chain affected the luminescence properties of these complexes.

The time-resolved decay lifetimes of these gold(I) complexes were tested to quantify the luminescence (Table S1 and Figs. S1–S6 in Supporting information). Surprisingly, yellow-green-emissive **1-Cl** exhibited an unexpectedly long lifetime of 42.80 ms at 492 nm; such a long lifetime is very rare in gold(I) complexes [49]. The solid or crystal of **1-Cl** showed a long afterglow after removing the UV light, exhibiting long-lifetime (millisecond scale) room temperature phosphorescence. The other complexes **2-Br**, **3-I**, **4-H** and **5-CCl** exhibited decay lifetimes of 21.75 μs, 7.04 μs, 27.57 μs, and 4.70 μs, respectively. Room temperature phosphorescence (RTP) properties were present in these complexes according to their microsecond lifetime range. Comparing the lifetimes of **1-Cl**, **2-Br** and **3-I**, we initially concluded that the halogen atoms influenced the lifetimes because of the heavy atom effect. In addition, the ultra-long lifetime of **1-Cl** and the shortest lifetime of **5-CCl** suggested that the oxygen atoms in the flexible chain were conducive to stabilize the triplet excited state and increase the lifetime.

As can be seen in Fig. 2, the prepared solids of these complexes emitted yellow-green (**1-Cl**), blue (**2-Br**), purple (**3-I**), cyan (**4-H**), and green (**5-CCl**) phosphorescence under irradiation with a 365 nm UV lamp. Their colors changed significantly after mechanical grinding, demonstrating mechanochromic properties. For example, the maximum emission peaks of complex **1-Cl** were located at 507 nm and 531 nm after grinding; the peaks in the short-wavelength range of 400–460 nm disappeared, and this was simultaneously accompanied by a change of the phosphorescent color from yellow-green to green. After treating with CH_2Cl_2 solvent, the emission peaks and luminescent color recovered, showing reversible phosphorescent mechanochromism. For the other two halogen-containing complexes, **2-Br** and **3-I**, broad emission peaks were found in the range of 400–700 nm after grinding; the initial emission peaks were obtained after solvent treatment, showing high-contrast phosphorescent blue-cyan-blue (**2-Br**) and purple-cyan-purple (**3-I**) mechanochromism. The reference complexes **4-H** and **5-CCl** exhibited similar reversible mechano-responsive behaviors, and a bright green phosphorescence was found after grinding. Their corresponding luminescence lifetimes of complexes **1-Cl**, **2-Br**, **3-I**, **4-H** and **5-CCl** after grinding and then after fuming are exhibited in Figs. S7–S11 (Supporting information).

Powder X-ray diffractometer (XRD) analysis was carried out to preliminarily explore the mechanism of phosphorescent mechanochromism. As shown in supporting information (Fig. S12 in Supporting information), strong and sharp diffraction peaks were detected in the prepared solid powders, indicating their highly ordered crystalline state. However, the diffraction peaks mostly disappeared after grinding, which suggested that the complexes were in a disordered amorphous state. After solvent treatment, these strong diffraction peaks appeared again, and the ordered crystalline states were obtained again. The powder XRD experiments indicated that the stimulus provided by the mechanical force caused a crystalline-to-amorphous transition. It was demonstrated that the intermolecular interactions present in the solids played a crucial role in their emission properties and mechanochromisms.

Subsequently, the emission properties of these gold(I) complexes in solutions were also studied. Normalized emission spectra of all the gold(I) complexes in pure DMF as well as 90% water fraction are shown in Fig. S13 (Supporting information). The complexes all exhibited extremely similar emission peaks in pure DMF. They were in the range of 365–500 nm with weak intensities, showing hardly any luminescence. Given that the solids all showed good luminescence properties, the aggregation-induced emission (AIE) properties of these complexes were then tested (Fig. 3). For three halogen-containing complexes, **1-Cl**, **2-Br** and **3-I**, when the water fraction (f_w) increased to a certain degree (f_w = 80% for **1-Cl**, f_w = 80% for **2-Br** and f_w = 60% for **3-I**), their solutions emitted a bright yellow light with emission peaks at 576 nm, 576 nm, and 568 nm, respectively.

Similar luminescent colors could be derived from the aurophilic interactions. The different degrees of aggregation indicated that the halogen atoms could affect the aggregation of the complexes. For the reference complexes, **4-H** exhibited similar aggregation-induced emission properties, while **5-CCl** showed the completely opposite emission characteristics. **4-H** started to aggregate and emitted bright yellow light at f_w = 80%, with the maximum emission peak at 580 nm; however, no naked eye observable luminescence was noticed in **5-CCl** during the entire aggregation process. These results indicated that the halogen atoms at the ends of the flexible chains would not fundamentally change the aggregation-induced emission effect, but they would completely change the

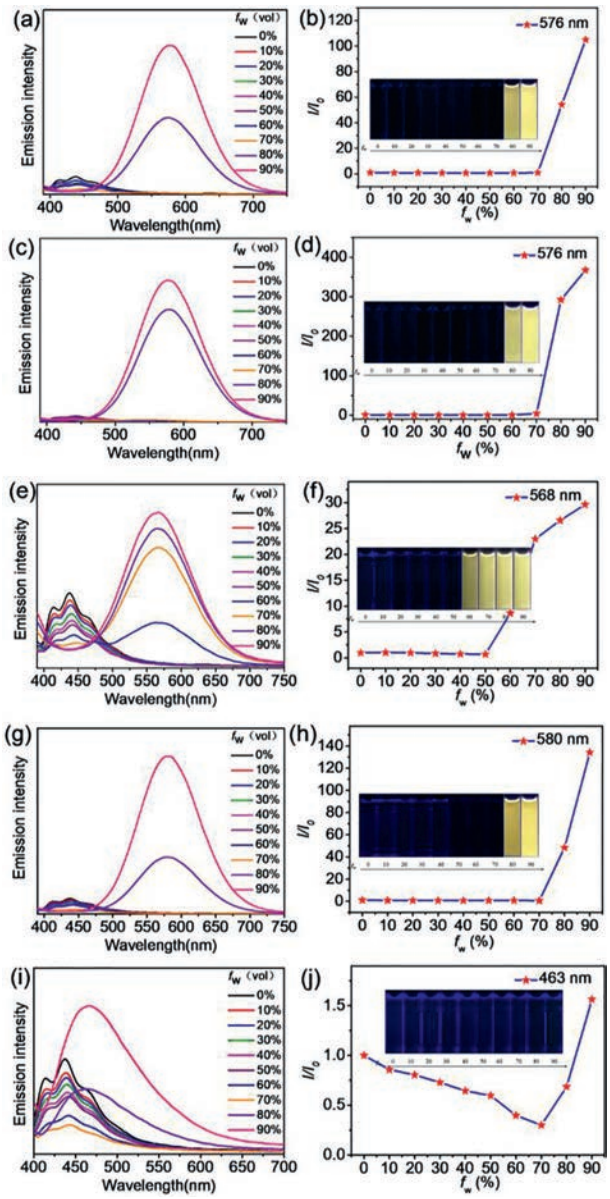

Fig. 3. PL spectra of **1-Cl** (a), **2-Br** (c), **3-I** (e), **4-H** (g), **5-CCl** (i) in DMF/H_2O mixtures with various water fractions (f_w) (concentration: 20 μmol/L, excitation wavelength: 365 nm). Changes in emission intensity of **1-Cl** (b), **2-Br** (d), **3-I** (f), **4-H** (h), **5-CCl** (j) in DMF/H_2O mixtures with different water contents. The insets show the corresponding photographs of gold(I) complexes (concentration: 20 μmol/L) in DMF/H_2O mixtures with different water contents under 365 nm UV light.

solid-state luminescence properties. In addition, these results also indicated that the gold(I) complexes had different aggregation-induced emission capabilities (Fig. S14 in Supporting information) because of the influence of the different halogen atoms and oxygen atoms.

To track the aggregation process, the absorption spectra in the DMF/H_2O mixtures with various water fractions were also tested (Fig. S15 in Supporting information). The absorption peaks for all the complexes were located at 200–300 nm in pure DMF, corresponding to the π-π^* transition (Fig. S13b). For the AIE complexes **1-Cl**, **2-Br**, **3-I** and **4-H**, red-shifted and broaden absorption peaks were observed when f_w increased to a certain degree, proving the formation of nanoaggregates. The dynamic light scattering (DLS) experiments showed that the formed nanoaggregates had an average particle size of ~100 nm (Fig. S16 in Supporting information). However, for the ACQ complex, **5-CCl**, no luminescent nanoaggregates formed with an excessively large average particle size after aggregation, and there was no significant intermolecular aurophilic interactions; thus, the AIE was not present in **5-CCl**. In addition, at f_w = 90%, a new absorption peak appeared at 324 nm, which could be attributed to intermolecular charge transfer (ICT). The ICT process also dissipated the energy of the complex, resulting in the absence of observable luminescence.

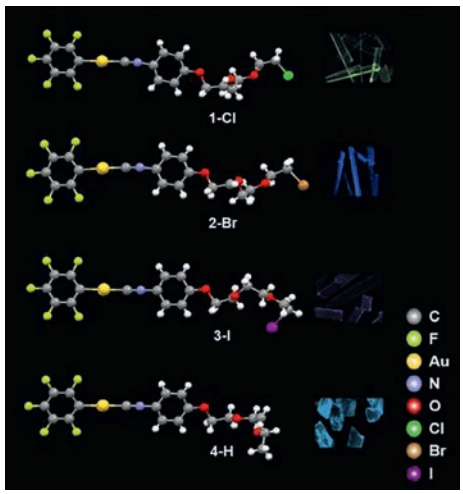

Fig. 4. Crystal structures of **1-Cl**, **2-Br**, **3-I** and **4-H**. The insets show the corresponding luminescence images of their crystals under 365 nm UV light.

In order to further explore the possible solid-state long-lifetime RTP mechanism, the crystal structures of complexes **1-Cl** (CCDC: 2008407), **2-B** (CCDC: 2012927), **3-I** (CCDC: 1958066) and **4-H** (CCDC: 2012926) were then established and analyzed (Fig. 4). For single molecules, the dihedral angles of the isocyanide phenyl and pentafluorophenyl groups were 15.13° (**1-Cl**), 15.43° (**2-Br**), 1.58° (**3-I**), and 6.00° (**4-H**), showing a coplanar conjugation. The head-to-head stacking patterns of **1-Cl** and **2-Br** were caused by intermolecular C–H···π and C–H···O interactions, respectively; while **3-I** and **4-H** adopted head-to-tail stacking with weak π-π interactions (Fig. S17 in Supporting information). Different distances of Au···Au were found (4.653 Å for **1-Cl**; 4.720 Å for **2-Br**; 3.532 and 4.558 Å for **3-I**; 4.170 and 5.014 Å for **4-H**), indicating no intermolecular aurophilic interaction.

Multiple hydrogen-bonding interactions were found between complexes, such as C–H···F interactions and C–H···O interactions, providing a rigid environment and limiting the change in molecular conformation. Among them, **1-Cl** possessed the greatest number and strongest C–H···F and C–H···O interactions (Fig. S18a in Supporting information). Each molecule was connected to the surrounding molecules *via* six C–H···F interactions. The compact stacking mode minimized the possibility of non-radiative transitions [50,51]. The strongest C–H···F (2.540, 2.543, 2.546 Å) and C–H···O (2.424 Å) interactions were found in **1-Cl**, while other complexes with relatively weaker hydrogen-bonding interactions (C–H···F: 2.584, 2.629 Å for **2-Br**; 2.527, 2.603, 2.612 Å for **3-I**; 2.552, 2.727 Å for **4-H**; C–H···O: 2.470, 2.706 Å for **2-Br**; 2.531 Å for **3-I**; 2.838, 2.845, 2.903, 2.966 Å for **4-H**). Stronger intermolecular interactions mean closer electronic communications and are more conducive to improving their luminescence lifetimes.

By analyzing the structure-property relationship, the introduction of heavy atoms in the flexible chains was determined to be beneficial for increasing the rate of intersystem crossing and enhancing the spin-orbit coupling effect. Halogen bonds were formed in **1-Cl** ($d_{Cl\cdots Cl}$ = 3.354 Å) and **2-Br** ($d_{Br\cdots Br}$ = 3.460 Å). In addition to the halogen atoms at the end of the flexible chains, there were also F···F interactions in **1-Cl** and **2-Br**, which were formed by fluorine atoms on the benzene rings ($d_{F\cdots F}$ = 2.878 Å (**1-Cl**), 2.915 Å

(**2-Br**)) (Fig. S19 in Supporting information). The head-to-tail structure of **3-I** increased the distance between iodine atoms, and there was no halogen bond interaction between molecules. However, **5-CCl** might have a poor crystallization ability because of the lack of oxygen atoms and multiple C–H···O interactions in the flexible chain, resulting in a failure to obtain its single crystal structure. On the whole, the intermolecular interactions played a decisive role in the solid luminescence properties and decay lifetimes of these gold(I) complexes.

In summary, three halogen-containing and two reference gold(I) complexes are designed and synthesized in this paper. By exploring the structure-property relationship, we find that multiple intermolecular interactions and compact molecular stacking are important factors for achieving long-lifetime RTP of gold(I) complexes. For complexes **1-Cl** and **5-CCl**, the presence of more oxygen atoms is beneficial to the formation of multiple hydrogen-bonding interactions, which contributes to increase the phosphorescence lifetime of **1-Cl**. By comparing their phosphorescence lifetimes of complexes **1-Cl**, **2-Br**, **3-I** and **4-H**, it is found that the introduction of halogen atoms does not necessarily increase the lifetime values of gold(I) complexes. However, the existence of chlorine atom seems to be helpful to realize long-lifetime RTP of gold(I) complexes. In the solid state, these complexes with tunable colors exhibit reversible phosphorescent mechanochromic properties. We also study the effect of the halogen and oxygen atoms on the aggregation-induced emission behaviors of gold(I) complexes and find that the different halogen atoms do not significantly change their AIE properties, but the absence of oxygen atoms in the flexible chain leads to the suppression of AIE in the complexes. Through crystal structure analysis, it is clearly demonstrated that intermolecular hydrogen-bonding interactions play a vital role in the photophysical properties of the complexes. In conclusion, this work provides a valuable reference for constructing novel functionalized materials with RTP, phosphorescent mechanochromism, and AIE characteristics.

Declaration of competing interest

The authors declare no conflict of interest.

Acknowledgments

The authors are grateful for the financial support from the National Natural Science Foundation of China (Nos. 22175069, 22061018, 21702079 and 21772054), the 111 Project (No. B17019), the Natural Science Foundation for Distinguished Young Scholars of Jiangxi Province (No. 20212ACB213003), and the Academic and Technical Leader Plan of Jiangxi Provincial Main Disciplines (No. 20212BCJ23004).

Supplementary materials

Supplementary material associated with this article can be found, in the online version, at doi:10.1016/j.cclet.2021.12.030.

References

[1] D. Li, W. Chen, S.H. Liu, X. Chen, J. Yin, Chin. Chem. Lett. 31 (2020) 2891–2896.
[2] W.K. Kwok, M.C. Tang, S.L. Lai, et al., Angew. Chem. Int. Ed. 59 (2020) 9684–9692.
[3] X. Liang, Z.P. Yan, H.B. Han, et al., Angew. Chem. Int. Ed. 57 (2018) 11316–11320.
[4] Y. Sun, F. Ding, Z. Chen, et al., Proc. Natl. Acad. Sci. U. S. A. 116 (2019) 16729–16735.
[5] F. Ding, Z. Chen, W.Y. Kim, et al., Chem. Sci. 10 (2019) 7023–7028.
[6] Z. Huang, Z. Bin, R. Su, et al., Angew. Chem. Int. Ed. 59 (2020) 9992–9996.
[7] L. Xu, J. Wang, Q. Luo, et al., Mater. Chem. Front. 4 (2020) 2389–2397.
[8] Y. Yin, Z. Chen, C. Fan, G. Liu, S. Pu, ACS Omega 4 (2019) 14324–14332.
[9] J. Luo, Z. Xie, J.W.Y. Lam, et al., Chem. Commun. (2001) 1740–1741.
[10] H. Lu, K. Wang, B. Liu, et al., Mater. Chem. Front. 3 (2019) 331–338.
[11] F. Ren, J. Shi, B. Tong, Z. Cai, Y. Dong, Mater. Chem. Front. 3 (2019) 2072–2076.
[12] H. Nie, K. Hu, Y. Cai, et al., Mater. Chem. Front. 1 (2017) 1125–1129.
[13] M. Yamaguchi, S. Ito, A. Hirose, K. Tanaka, Y. Chujo, Mater. Chem. Front. 1 (2017) 1573–1579.
[14] R. Zhang, Y. Duan, B. Liu, Nanoscale 11 (2019) 19241–19250.
[15] S. Jiang, L. Meng, W. Ma, et al., Chin. Chem. Lett. 32 (2021) 1037–1040.
[16] W. Qiao, P. Yao, Y. Chen, et al., Mater. Chem. Front. 4 (2020) 2688–2696.
[17] Y. Takeda, P. Data, S. Minakata, Chem. Commun. 56 (2020) 8884–8894.
[18] W. Yang, Y. Yang, Y. Qiu, et al., Mater. Chem. Front. 4 (2020) 2047–2053.
[19] Z. Chen, J. Zhang, M. Song, et al., Chem. Commun. 51 (2015) 326–329.
[20] Z. Chen, Y. Yin, S. Pu, S.H. Liu, Dye. Pigment. 184 (2021) 108814.
[21] Y. Yin, Z. Chen, R.H. Li, et al., Inorg. Chem. 60 (2021) 9387–9393.
[22] M. Yang, I.S. Park, Y. Miyashita, K. Tanaka, T. Yasuda, Angew. Chem. Int. Ed. 59 (2020) 13955–13961.
[23] Z. Chen, Y. Nie, S.H. Liu, RSC Adv. 6 (2016) 73933–73938.
[24] F. Lin, Y. Feng, X. Liu, et al., Mater. Chem. Front. 4 (2020) 1492–1499.
[25] S. Saotome, K. Suenaga, K. Tanaka, Y. Chujo, Mater. Chem. Front. 4 (2020) 1781–1788.
[26] Z. Chen, J.H. Tang, W. Chen, et al., Organometallics 38 (2019) 4244–4249.
[27] Q. Liao, Q. Gao, J. Wang, et al., Angew. Chem. Int. Ed. 59 (2020) 9946–9951.
[28] J. Wang, Z. Chai, J. Wang, et al., Angew. Chem. Int. Ed. 58 (2019) 17297–17302.
[29] Y. Xie, Y. Ge, Q. Peng, et al., Adv. Mater. 29 (2017) 1606829.
[30] T. Jadhav, B. Dhokale, S.M. Mobin, R. Misra, J. Mater. Chem. C 3 (2015) 9981–9988.
[31] Y. Tani, M. Terasaki, M. Komura, T. Ogawa, J. Mater. Chem. C 7 (2019) 11926–11931.
[32] Y. Dong, J. Zhang, A. Li, et al., J. Mater. Chem. C 8 (2020) 894–899.
[33] X.Y. Wang, J. Zhang, Y.B. Dong, et al., Dye. Pigment. 156 (2018) 74–81.
[34] Z. Chen, G. Liu, S. Pu, S.H. Liu, Dye. Pigment. 152 (2018) 54–59.
[35] W. Qiu, P.A. Gurr, G.d. Silva, G.G. Qiao, Polym. Chem. 10 (2019) 1650–1659.
[36] C.L. Anderson, N. Dai, S.J. Teat, et al., Angew. Chem. Int. Ed. 58 (2019) 17978–17985.
[37] J.X. Chen, J.Y. Wang, Q.C. Zhang, Z.N. Chen, Inorg. Chem. 56 (2017) 13257–13266.
[38] X. Zhang, L.Y. Zhang, J.Y. Wang, F.R. Dai, Z.N. Chen, J. Mater. Chem. C 8 (2020) 715–720.
[39] T. Lu, J.Y. Wang, D. Tu, et al., Inorg. Chem. 57 (2018) 13618–13630.
[40] X.Y. Wang, Y.X. Hu, X.F. Yang, et al., Org. Lett. 21 (2019) 9945–9949.
[41] K.Y. Zhao, H.T. Mao, L.L. Wen, et al., J. Mater. Chem. C 6 (2018) 11686–11693.
[42] J. Li, L. Wang, Z. Zhao, et al., Angew. Chem. Int. Ed. 59 (2020) 8210–8217.
[43] W. Zhu, L. Fan, Dye. Pigment. 76 (2008) 663–668.
[44] Z. Chen, G. Liu, S. Pu, S.H. Liu, Dye. Pigment. 143 (2017) 409–415.
[45] Y. Dong, F. Zhu, Z. Chen, J. Yin, S.H. Liu, Mater. Chem. Front. 3 (2019) 1866–1871.
[46] S. Cheng, Z. Chen, Y. Yin, Y. Sun, S. Liu, Chin. Chem. Lett. 32 (2021) 3718–3732.
[47] T. Seki, S. Kurenuma, H. Ito, Chem. Eur. J. 19 (2013) 16214–16220.
[48] N. Mirzadeh, S.H. Privér, A.J. Blake, H. Schmidbaur, S.K. Bhargava, Chem. Rev. 120 (2020) 7551–7591.
[49] X.Y. Wang, Y. Yin, J. Yin, Z. Chen, S.H. Liu, Dalton Trans. 50 (2021) 7744–7749.
[50] J. Mei, N.L.C. Leung, R.T.K. Kwok, J.W.Y. Lam, B.Z. Tang, Chem. Rev. 115 (2015) 11718–11940.
[51] F. Würthner, T.E. Kaiser, C.R. Saha-Möller, Angew. Chem. Int. Ed. 50 (2011) 3376–3410.